JVI Journals.ASM.org

Tom70 Mediates Sendai Virus-Induced Apoptosis on Mitochondria

Bo Wei,[a] Ye Cui,[a] Yuefeng Huang,[a] Heng Liu,[a] Lin Li,[a] Mi Li,[b] Kang-Cheng Ruan,[a] Qin Zhou,[b] Chen Wang[a]

State Key Laboratory of Cell Biology, Institute of Biochemistry and Cell Biology, Shanghai Institutes for Biological Sciences, Chinese Academy of Sciences, Shanghai, China[a]; The Division of Molecular Nephrology and the Creative Training Center for Undergraduates, The M.O.E. Key Laboratory of Laboratory Medical Diagnostics, The College of Laboratory Medicine, Chongqing Medical University, Chongqing, China[b]

ABSTRACT

Virus infection triggers immediate innate immune responses. Apoptosis represents another effective means to restrict virus invasion, besides robust expression of host cytokines and chemokines. IRF3 was recently demonstrated to be indispensable for Sendai virus (SeV)-induced apoptosis, but the underlying mechanism is not fully understood. Here we report that a dynamic protein complex, Tom70/Hsp90/IRF3/Bax, mediates SeV-induced apoptosis. The cytosolic proapoptotic protein Bax interacts specifically with IRF3 upon virus infection. The mitochondrial outer membrane protein Tom70 recruits IRF3 to mitochondria via Hsp90. Consequently, the relocation of Bax onto mitochondria induces the leakage of cytochrome *c* into the cytosol and initiates the corresponding apoptosis. Interestingly, IKK-i is essential for this apoptosis, whereas TBK1 is dispensable. Collectively, our study characterizes a novel protein complex that is important for SeV-induced apoptosis.

IMPORTANCE

Apoptosis is an effective means of sacrificing virus-infected cells and restraining the spread of virus. In this study, we demonstrate that IRF3 associates with Bax upon virus infection. Tom70 recruits this protein complex to the mitochondrial outer membrane through Hsp90, which thus induces the release of cytochrome *c* into the cytosol, initiating virus-induced apoptosis. Interestingly, IKK-i plays an essential role in this activation. This study uncovers a novel mechanism of SeV-induced apoptosis.

Pathogen-associated molecular patterns (PAMPs) are sensed by germ line-encoded pattern recognition receptors (PRRs) in the innate immunity. Virus nucleic acids are predominantly recognized by Toll-like receptors (TLR3 for double-stranded RNA [dsRNA], TLR7 for single-stranded RNA [ssRNA], and TLR9 for CpG DNA) in the endosome and by retinoic acid-inducible gene I (RIG-I), melanoma differentiation-associated gene 50 (MDA5), cyclic GMP-AMP synthase DNA (cGAS), and other receptors in the cytosol (1, 2). These receptors trigger several cascades of signal transduction pathways, ultimately activating the critical transcription factors nuclear factor κB (NF-κB) and interferon regulatory factor 3 (IRF3), inducing the robust expression of type I interferons (IFNs), other cytokines, and chemokines (3).

The mitochondrion is the "powerhouse" of the cell and is essential for ATP synthesis, fatty acid synthesis, and calcium/iron homeostasis. In addition, mitochondria are firmly established as the critical initiators and transducers of apoptosis, or programmed cell death (4). Apoptosis is essential for tissue homeostasis, for instance, in the development of *Caenorhabditis elegans* and the negative/positive selection of T lymphocytes, whereas abnormalities in apoptosis are responsible for pathological diseases, such as cancer, autoimmune syndromes, and neurodegenerative diseases (Alzheimer's disease, Parkinson's disease, and Huntington's disease) (5–8). Notably, apoptosis is another effective means to restrict the spread of pathogens by sacrificing virus-infected host cells (9). For example, nonstructural protein 1 (NS1) of influenza virus can directly trigger apoptosis via multiple mechanisms (10, 11). PKR, a serine/threonine protein kinase induced by interferon, phosphorylates eIF2-α and attenuates overall protein translation, thus triggering apoptosis (12). In contrast, many viruses encode proteins to antagonize apoptosis, such as the Kaposi's sarcoma-associated herpesvirus (KSHV)-encoded viral FLCE inhibitory protein (vFLIP), the KSHV-encoded viral Bcl-2 protein (KS-Bcl-2), and African swine fever virus-encoded LMW5-HL (13–15). It is important to understand the roles of mitochondria in virus-induced apoptosis and to elucidate the relevant molecular mechanisms.

Most mitochondrial proteins are encoded by the nuclear genome and synthesized in the cytosol as preproteins, except for a few mitochondrion-encoded proteins. The translocase of outer membrane (TOM) complex, an ~400-kDa core complex in the mitochondrial outer membrane, is responsible for the recognition and translocation of the mitochondrial preproteins from the cytosol into the mitochondria (16, 17). Tom20 and Tom70 are characterized as two major import receptors in the TOM complex that mediate recognition via different mechanisms. Tom20 recognizes the classical N-terminal mitochondrion-targeting signal peptides, which are positively charged amphipathic helices and are found in most mitochondrial preproteins. In contrast, the Tom70 receptor interacts specifically with the chaperone Hsp90, which then recruits its client proteins to the mitochondria (18, 19).

Seminal studies recently identified the mitochondrial outer membrane protein MAVS/IPS-1/VISA/Cardiff as an essential adaptor for RIG-I/Mda5 signal transduction during RNA virus

Received 10 October 2014 **Accepted** 12 January 2015

Accepted manuscript posted online 21 January 2015

Citation Wei B, Cui Y, Huang Y, Liu H, Li L, Li M, Ruan K-C, Zhou Q, Wang C. 2015. Tom70 mediates Sendai virus-induced apoptosis on mitochondria. J Virol 89:3804–3818. doi:10.1128/JVI.02959-14.

Editor: R. M. Sandri-Goldin

Address correspondence to Qin Zhou, zhouqin@cqmu.edu.cn, or Chen Wang, cwang01@sibcb.ac.cn.

doi:10.1128/JVI.02959-14

infection (20–23). Our recent study characterized Tom70 as an important adaptor linking MAVS to TBK1/IRF3 activation, thus establishing a novel function of Tom70 in innate immunity (24). Unexpectedly, Hiscott et al. demonstrated that IRF3 could also mediate Sendai virus (SeV)-induced apoptosis, which is a nonredundant mechanism to effectively protect the host from virus infection (25). Notably, this apoptotic function of IRF3 is independent of its activity in innate immunity signaling (25). How IRF3 induces apoptosis during virus infection remains an intriguing question.

In this study, we show that the Tom70/Hsp90/IRF3 protein complex is important for SeV-induced apoptosis. Depletion of either Tom70, Hsp90, or IRF3 via RNA interference (RNAi) markedly attenuates SeV-induced apoptosis. Mechanistically, IRF3 interacts with both Hsp90 and the proapoptotic protein Bax in the cytosol, and these are translocated to mitochondria upon SeV infection. The clamp domain (R192) of Tom70 interacts with the C-terminal motif (EEVD) of Hsp90, thereby recruiting Hsp90/IRF3/Bax to mitochondria. Upon binding to IRF3, Bax dissociates from the antiapoptotic molecule Bcl-2 and interacts with the proapoptotic protein Bak on mitochondria, thus forming the mitochondrial outer membrane pore and promoting the release of cytochrome *c* from mitochondria into the cytosol. Collectively, the data in our study characterize a novel protein complex that is important for SeV-induced apoptosis, shedding new light on how IRF3 modulates SeV-induced apoptosis.

MATERIALS AND METHODS

Antibodies and reagents. The antibody against Tom70 was described previously (24). Antibodies obtained from commercial sources were as follows: anti-hemagglutinin (anti-HA), anti-Myc, anti-IRF3, anti-Bcl-2, anti-Tom20 (human), and anti-poly(ADP-ribose) polymerase (anti-PARP) were from Santa Cruz; anti-MAVS, anti-caspase-3, anti-caspase-9, anti-Bax, and anti-IKK-i were from Cell Signaling Technology; anti-Flag, anti-β-actin, and anti-tubulin were from Sigma; anti-Hsp90 and anti-Tom20 (mouse) were from Proteintech; anti-cytochrome *c* was from BD; anti-TBK1 and anti-COX IV were from Abcam; and anti-Bak was from Millipore. EZview red protein G affinity gel was purchased from Sigma. Inhibitors obtained from commercial sources were as follows: Z-VAD-FMK, Z-LEHD-FMK, and tumor necrosis factor alpha (TNF-α) were from R&D, cycloheximide (CHX) and a protease inhibitor cocktail were from Sigma, BX-795 was from Merck Millipore, radicicol (RA) was from Sigma, and geldanamycin (GA) was from TCI.

Cell culture and transfection. Human embryonic kidney 293 (HEK293), human embryonic kidney 293T (HEK293T), mouse embryonic fibroblast (MEF), and *irf3*$^{-/-}$ MEF cells were cultured in Dulbecco's modified Eagle's medium (DMEM; Gibco) plus 10% fetal bovine serum (FBS; Gibco) supplemented with 1% penicillin-streptomycin (Gibco) at 37°C and 5% CO_2. Transient transfections of indicated plasmids and small interfering RNAs (siRNAs) were performed with Lipofectamine 2000 (Invitrogen) following the manufacturer's instructions.

Plasmids. Human full-length IRF3, TBK1, Hsp90, MAVS, and Tom70 constructs were described previously (24). The cDNA encoding Bax and Bak was a gift from Mian Wu (University of Science and Technology of China). The cDNA encoding NS3/4A of hepatitis C virus (HCV) was a gift from Jing Zhong (The Shanghai Pasteur Institute, Chinese Academy of Sciences). Point mutants of Tom70 (R192A and K195A) were generated by using a QuikChange XL site-directed mutagenesis method. Hsp90 (M4) and Hsp90 (M2) had the last four amino acids (EEVD) of the C terminus changed to AAAA and EEAA, respectively. All Tom70 siRNA-resistant constructs were generated by introducing silent mutations into the Tom70 siRNA target sequence (1453-GCGCTGACGGACCAGCAA-1470). All Hsp90 siRNA-resistant constructs were generated by introducing silent mutations into the Hsp90 siRNA target sequence (1181-GTGA CAAAAAAAAAAAAAG-1200). All constructs were confirmed by sequencing.

siRNAs. All the siRNAs (GenePharma) were transfected using Lipofectamine 2000. HEK293 cells were plated in 12-well or 6-well plates in antibiotic-free growth medium. At about 40% confluence, 40 to 80 pmol of siRNA duplex was transfected into cells. The medium was replaced with fresh growth medium at 6 h posttransfection. To determine the efficiency of protein knockdown, cells were lysed and immunoblotted with the indicated antibodies at 48 h posttransfection.

The siRNA sequences were as follows: negative-control (NC) siRNA, 5′-UUCUCCGAAGGUGUCACGUTT-3′; Bax siRNA, 5′-UGAGCGAG UGUCUCAAGCGCA-3′; Bak siRNA, 5′-CCGACGCUAUGACUCAGA GTT-3′; Tom70 siRNA, 5′-GGCAUUAACAGAUCAACAATT-3′; Tom20 siRNA, 5′-CAAGUUACCUGACCUUAAATT-3′; Hsp90 siRNA, 5′-ACA AGAAGAAGAAGAAGAATT-3′; TBK1 siRNA, 5′-GACAGAAGUUGU GAUCACATT-3′; MAVS siRNAs, 5′-CCACCUUGAUGCCUGUGAAT T-3′ and 5′-CAGAGGAGAAUGAGUAUAATT-3′; IKK-i siRNAs, 5′-AC AGAAGCAUCCAGCAGAUTT-3′ and 5′-GGAGAUCAUGUACCGGA UCTT-3′; and IRF3 siRNAs, 5′-AGACAUUCUGGAUGAGUUATT-3′, 5′-GGAGGAUUUCGGAAUCUUCTT-3′, and 5′-AAUCAGAUCUACA AUGAAGGG-3′.

Subcellular fractionation. HEK293 cells or MEF cells (2×10^7) were harvested and washed with ice-cold phosphate-buffered saline (PBS) (Ca^{2+}-free). The cells were resuspended and homogenized in mitochondrial buffer (210 mM sucrose, 70 mM mannitol, 1 mM EDTA, 1 mM EGTA, 1.5 mM $MgCl_2$, 10 mM HEPES [KOH] [pH adjusted to 7.2], protease inhibitor cocktail). The homogenate was centrifuged at 1,000 × *g* and 4°C for 10 min. The nuclei and intact cells were discarded. The supernatant was collected, centrifuged at 5,000 × *g* and 4°C for 15 min, and then washed with mitochondrial buffer once. The mitochondria were contained in the pellet. The pellet was lysed and analyzed by SDS-PAGE and immunoblotting.

Immunoblotting and immunoprecipitation. Cells were collected and washed with ice-cold PBS and then lysed in RIPA buffer (50 mM Tris, pH 7.4, 150 mM NaCl, 1 mM EDTA, 1 mM EGTA, 0.5% NP-40, 1 mM Na_3VO_4, 1 mM β-glycerophosphate, 1 mM phenylmethylsulfonyl fluoride [PMSF], protease inhibitor cocktail) for immunoprecipitation or in RIPA buffer plus 0.05% SDS for immunoblotting. After centrifugation for 15 min at 12,000 × *g*, the supernatant was removed. For immunoprecipitation, about 1 μg of antibody was added to each cell lysate and then incubated overnight at 4°C. After addition of protein G beads, the incubation was continued for 4 h. The beads were washed three times with RIPA buffer, and bound protein was eluted with SDS loading buffer by boiling for 5 min. The immunoprecipitate or whole-cell lysate was analyzed by SDS-PAGE and transferred to a polyvinylidene difluoride (PVDF) membrane (Millipore). Immunoblots were probed with the indicated antibodies. The bound antibodies were visualized by using a Super Signal West Pico ECL kit (Pierce).

Confocal imaging. MEF cells were plated onto coverslips (Fisher) in 12-well plates and transfected with the indicated siRNAs. The coverslips with the cells were washed once with PBS and fixed in 4% paraformaldehyde in PBS for 15 min. Cells were permeabilized for 15 min in 0.2% Triton X-100 in PBS and blocked for 60 min in 5% bovine serum albumin (BSA) in PBS at room temperature. The cells were then incubated with a primary antibody for 60 min at room temperature or overnight at 4°C. After washing three times in PBS, cells were incubated with Alexa 488-conjugated goat anti-mouse IgG (Life Technologies) for 1 h at room temperature. Nuclei were counterstained with DAPI (4′,6-diamidino-2-phenylindole; Sigma) for 2 min. The coverslips were then washed extensively and mounted by use of Aqua-Poly/Mount reagent (Polysciences). Imaging of the cells was performed at room temperature, using a confocal microscope (TCS SP2 ACBS; Leica) with a 63× (numerical aperture = 1.4) oil immersion objective. The acquiring software was TCS (Leica, Solms, Germany).

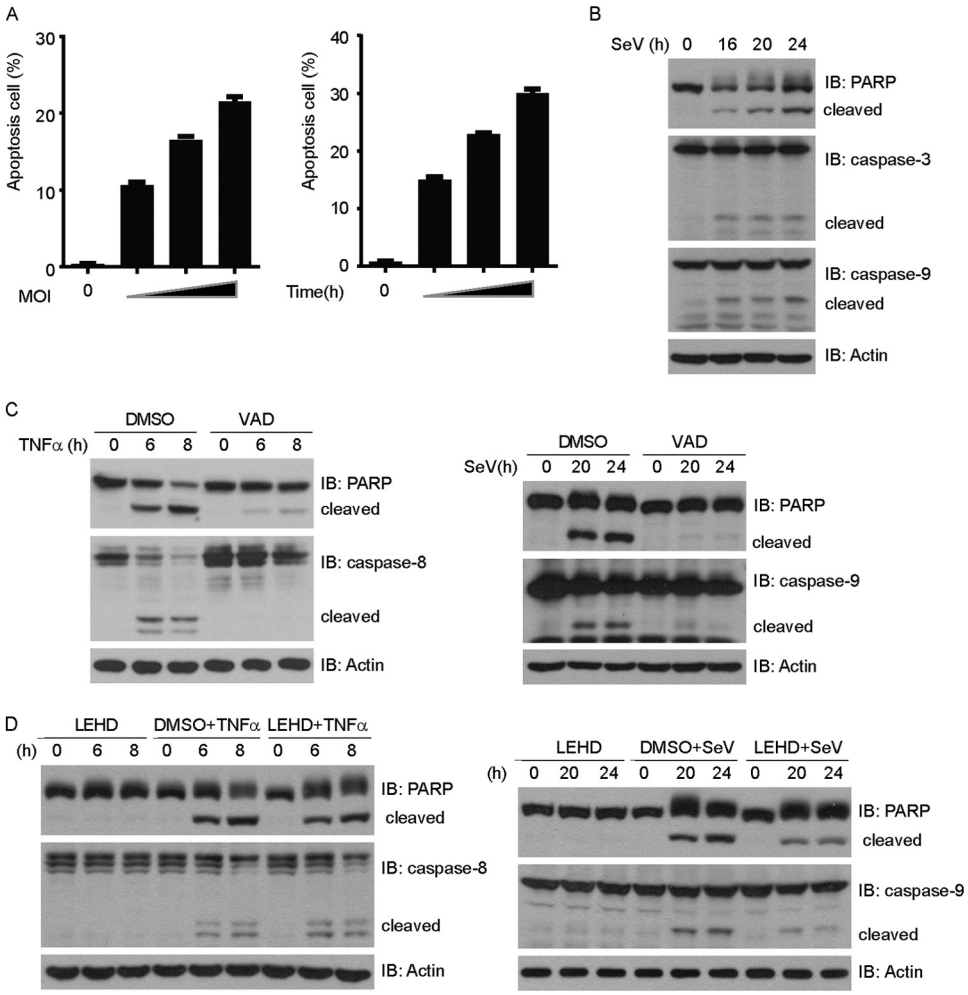

FIG 1 Sendai virus-induced apoptosis depends on caspase-9. (A) HEK293 cells were infected with Sendai virus at an MOI of 0.4, 0.8, or 1.2 for 24 h (left) or at an MOI of 1 for 18, 21, or 24 h (right). Cell death was quantified using annexin V/PI double staining on flow cytometry. (B) HEK293 cells were infected with Sendai virus for the indicated times. Cell lysates were resolved by SDS-PAGE and then immunoblotted (IB) with the indicated antibodies. (C) (Left) HEK293 cells were treated with TNF-α (10 ng/ml) and CHX (10 ng/ml) plus Z-VAD-FMK (2 μM) for the indicated times. (Right) HEK293 cells were infected with Sendai virus plus Z-VAD-FMK (2 μM) for the indicated times. Cell lysates were collected for Western blot analysis with the indicated antibodies. (D) (Left) HEK293 cells were treated with TNF-α (10 ng/ml) and CHX (10 ng/ml) plus Z-LEHD-FMK (2 μM) for the indicated times. (Right) HEK293 cells were infected with Sendai virus plus Z-LEHD-FMK (2 μM) for the indicated times. Cell lysates were collected for immunoblot analysis with the indicated antibodies.

Rescue experiments. HEK293 cells were first treated with the indicated siRNAs for 24 h and then transfected again with the indicated siRNA-resistant plasmids for 24 h, followed by Sendai virus infection.

Virus infection. HEK293 and MEF cells were infected with Sendai virus (strain Cantell; multiplicity of infection [MOI] = 1) in serum-free DMEM at 80% cell confluence. Following adsorption for 2 h at 37°C and 5% CO_2, the medium was removed, and cells were washed with DMEM once and cultured with DMEM plus 10% FBS for the indicated periods. The infectivity titer of the stock virus was 320 hemagglutinating units (HAU)/ml.

Annexin V staining and flow cytometry. After treatment or no treatment, cells were collected and stained with annexin V and propidium iodide (PI) (Molecular Probes) according to the manufacturer's instructions. Cell apoptosis was detected using a FACSCalibur flow cytometer (BD Biosciences), and the data were analyzed with FlowJo software (Ashland, OR).

OIRD method. All recombinant proteins were purified from *Escherichia coli* BL21. The oblique-incidence reflectivity difference (OIRD) method was performed as described previously (26, 27). BSA and recombinant Hsp90 proteins were placed on processed glass chips by use of Microarray Spotter and then immobilized for 12 h at 25°C. The chips were blocked with BSA for 1 h and then incubated with recombinant Tom70 proteins for 1 h at 25°C. Lastly, OIRD detection was carried out.

Statistics. Student's *t* test was used for statistical analysis. *P* values of <0.05 were considered statistically significant.

RESULTS

Sendai virus induces apoptosis that is dependent on caspase-9. Consistent with previous reports, persistent SeV infection resulted in robust cell apoptosis (Fig. 1A). One of the salient features of apoptosis is the activation of the aspartate-specific proteases, or caspases (28). PARP, a zinc finger protein with important roles in DNA repair and DNA replication, is one of the target substrates of activated caspases (29). SeV infection triggered the cleavage of caspase-3 and PARP. In addition, the initiator caspase-9 was cleaved and activated (Fig. 1B). In contrast, treatment with TNF-α

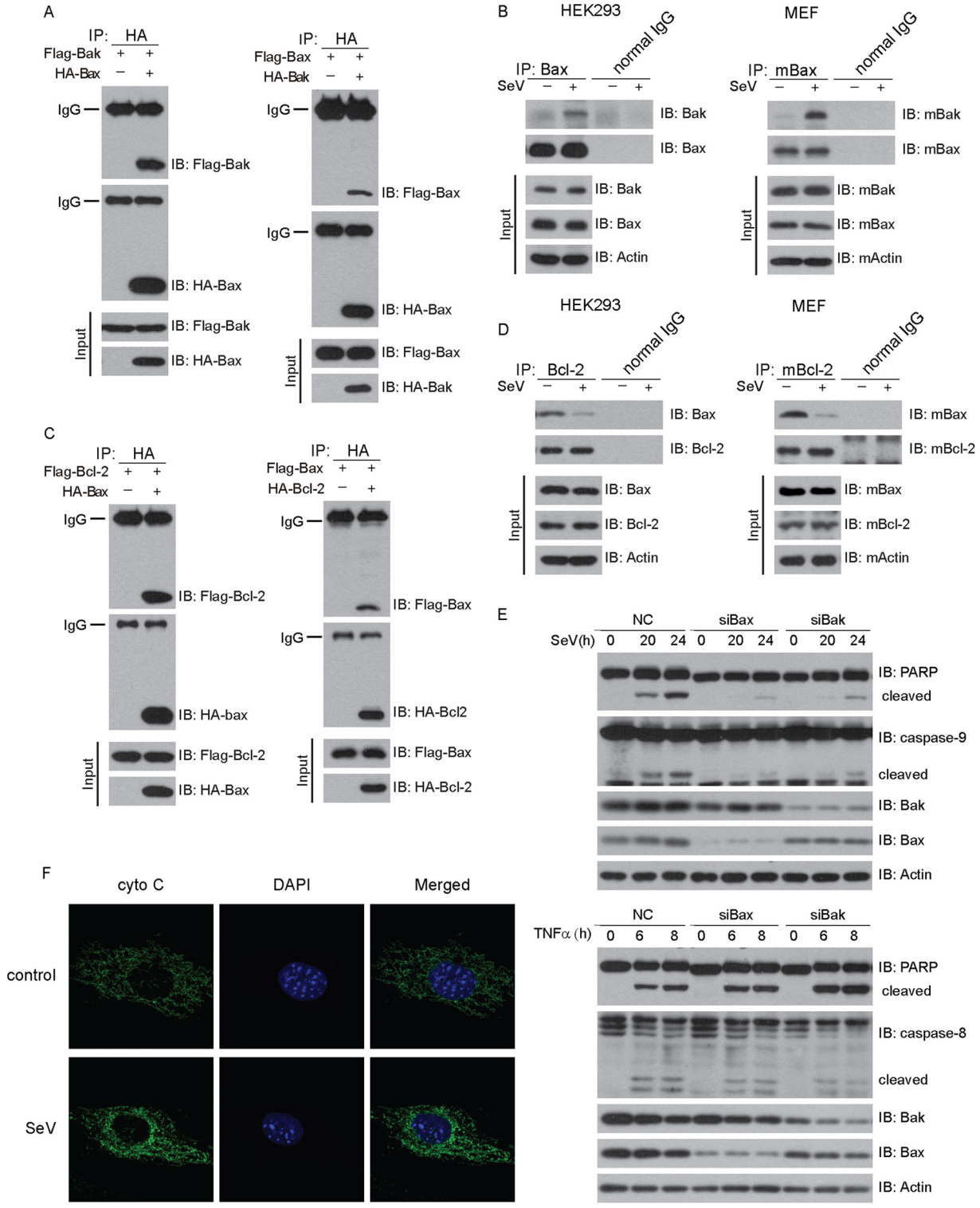

FIG 2 Sendai virus activates intrinsic mitochondrial apoptosis. (A and C) HEK293T cells were cotransfected with Bak and Bax (A) or Bcl-2 and Bax (C) for 36 h and then subjected to immunoprecipitation (IP) with anti-HA antibody. The immunoprecipitates were analyzed by immunoblotting with the indicated antibodies. (B and D) HEK293 cells or MEF cells were challenged with SeV for 24 h, and then cell lysates were subjected to immunoprecipitation with normal IgG or anti-Bax antibody. The immunoprecipitates were analyzed by immunoblotting with the indicated antibodies. (E) Host cells were transfected with negative-control (NC), Bax, or Bak siRNA and then infected with SeV (upper panel) or treated with TNF-α (10 ng/ml) and CHX (10 ng/ml) (lower panel) for the indicated times. Cell lysates were collected for Western blot analysis with the indicated antibodies. (F) MEF cells were infected with SeV for 24 h, stained with anti-cytochrome *c* antibody, and then imaged by confocal microscopy.

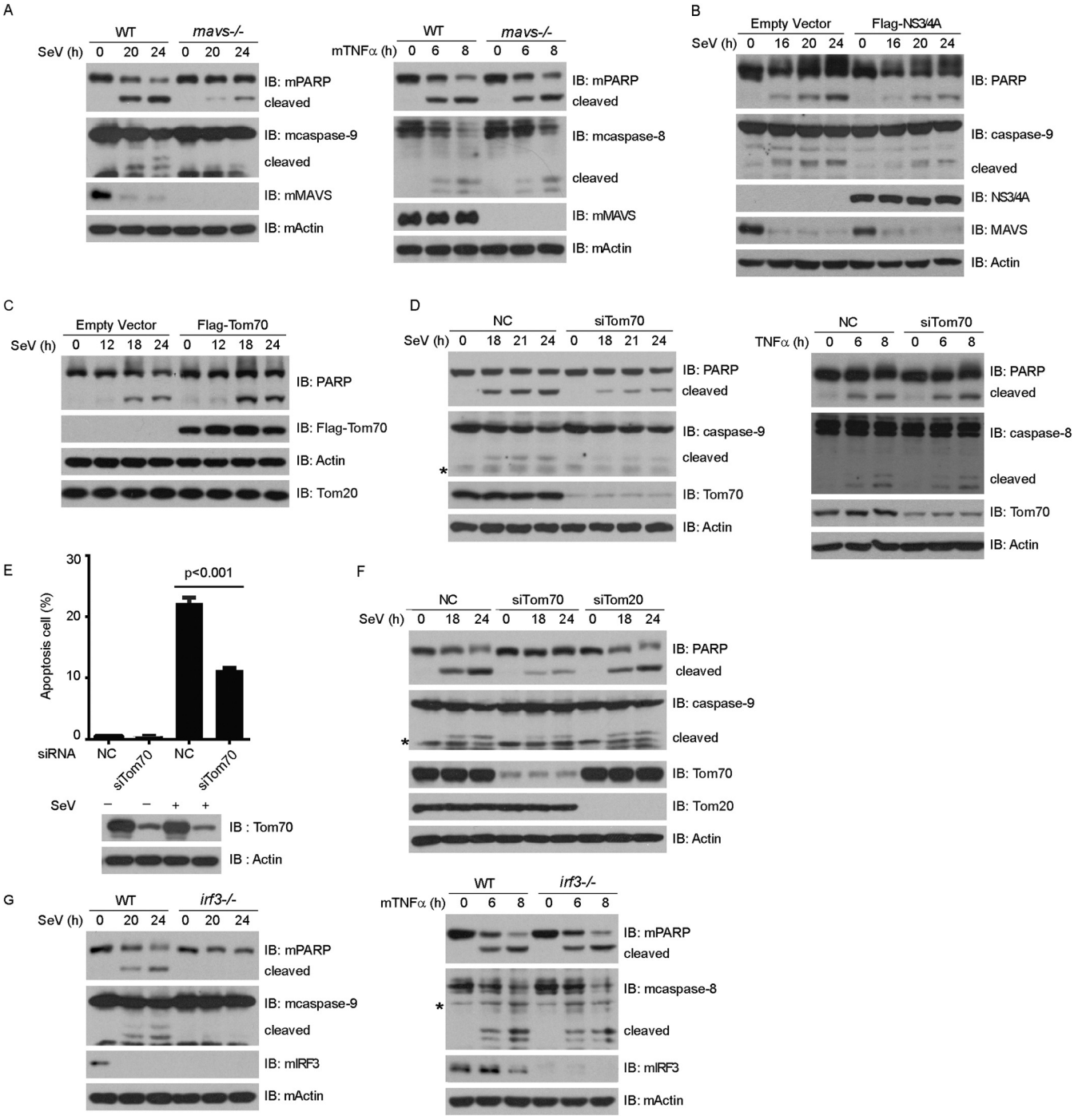

FIG 3 MVAS, Tom70, and IRF3 mediate Sendai virus-induced apoptosis. (A) Wild-type (WT) and *mavs*$^{-/-}$ MEF cells were infected with SeV (MOI = 3) (left) or treated with TNF-α (10 ng/ml) and CHX (10 ng/ml) (right) for the indicated times. Cell lysates were collected for Western blot analysis with the indicated antibodies. (B and C) HEK293 cells were transfected with empty vector, Flag-NS3/4A (B), or Flag-Tom70 (C) for 24 h and then infected with SeV for the indicated times. Cell lysates were collected for Western blot analysis. (D) HEK293 cells were transfected with NC or Tom70 siRNA and then infected with SeV (left) or treated with TNF-α (10 ng/ml) and CHX (10 ng/ml) (right) for the indicated times. Cell lysates were collected for Western blot analysis with the indicated antibodies. (E and F) HEK293 cells were transfected with the indicated siRNAs and infected with SeV. (E) Cell apoptosis was quantified using annexin V staining and flow cytometry. (F) Cell lysates were collected for Western blot analysis with the indicated antibodies. (G) Wild-type (WT) and *irf3*$^{-/-}$ MEF cells were infected with SeV (MOI = 3) (left) or treated with mTNF-α (10 ng/ml) and CHX (10 ng/ml) (right) for the indicated times. Cell lysates were collected for Western blot analysis with the indicated antibodies. NC, negative-control siRNA; *, nonspecific band.

plus cycloheximide (CHX) triggered the cleavage of caspase-8 and PARP (Fig. 1C).

Z-VAD-FMK, a broad-spectrum inhibitor of the caspases, not only inhibited SeV-induced apoptosis but also inhibited TNF-α-induced apoptosis (Fig. 1C). Interestingly, Z-LEHD-FMK, a specific inhibitor of caspase-9, apparently could inhibit SeV-induced apoptosis (cleavage of caspase-9 and PARP), whereas it failed to inhibit TNF-α-induced apoptosis (cleavage of caspase-8 and

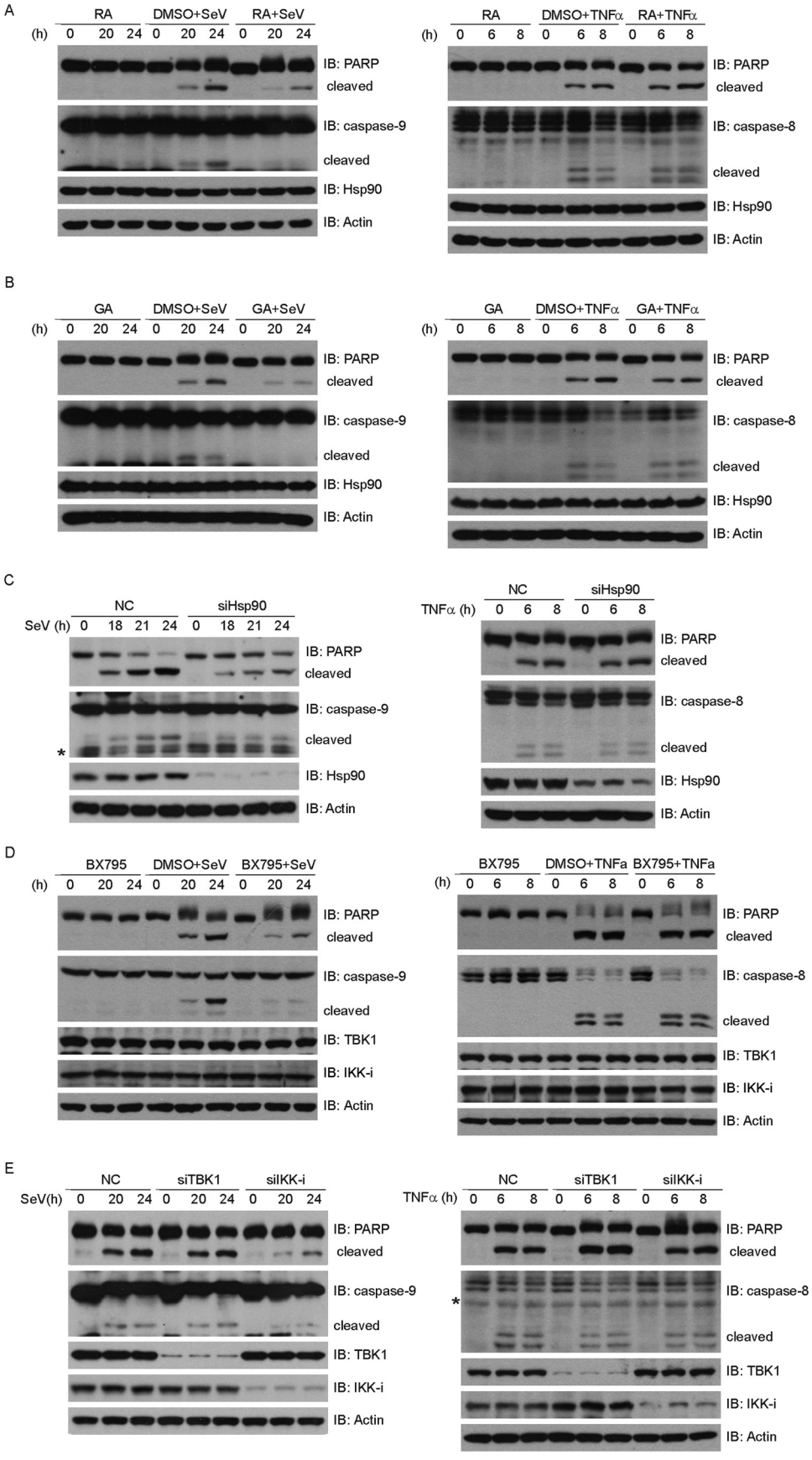
A
RA
DMSO+SeV
RA+SeV
(h) 0 20 24 0 20 24 0 20 24
IB: PARP
cleaved
IB: caspase-9
cleaved
IB: Hsp90
IB: Actin
RA
DMSO+TNFα
RA+TNFα
(h) 0 6 8 0 6 8 0 6 8
IB: PARP
cleaved
IB: caspase-8
cleaved
IB: Hsp90
IB: Actin
B
GA
DMSO+SeV
GA+SeV
(h) 0 20 24 0 20 24 0 20 24
IB: PARP
cleaved
IB: caspase-9
cleaved
IB: Hsp90
IB: Actin
GA
DMSO+TNFα
GA+TNFα
(h) 0 6 8 0 6 8 0 6 8
IB: PARP
cleaved
IB: caspase-8
cleaved
IB: Hsp90
IB: Actin
C
NC
siHsp90
SeV (h) 0 18 21 24 0 18 21 24
IB: PARP
cleaved
IB: caspase-9
cleaved
*
IB: Hsp90
IB: Actin
NC
siHsp90
TNFα (h) 0 6 8 0 6 8
IB: PARP
cleaved
IB: caspase-8
cleaved
IB: Hsp90
IB: Actin
D
BX795
DMSO+SeV
BX795+SeV
(h) 0 20 24 0 20 24 0 20 24
IB: PARP
cleaved
IB: caspase-9
cleaved
IB: TBK1
IB: IKK-i
IB: Actin
BX795
DMSO+TNFa
BX795+TNFa
(h) 0 6 8 0 6 8 0 6 8
IB: PARP
cleaved
IB: caspase-8
cleaved
IB: TBK1
IB: IKK-i
IB: Actin
E
NC
siTBK1
siIKK-i
SeV(h) 0 20 24 0 20 24 0 20 24
IB: PARP
cleaved
IB: caspase-9
cleaved
IB: TBK1
IB: IKK-i
IB: Actin
NC
siTBK1
siIKK-i
TNFα (h) 0 6 8 0 6 8 0 6 8
IB: PARP
cleaved
*
IB: caspase-8
cleaved
IB: TBK1
IB: IKK-i
IB: Actin

PARP) (Fig. 1D). These results suggest that SeV-induced apoptosis is dependent on caspase-9.

Sendai virus activates intrinsic mitochondrial apoptosis. Intrinsic mitochondrial apoptosis is initiated by the release of cytochrome *c*, an essential component of the respiratory chains localized in the mitochondrial intermembrane spaces, followed by the formation of the apoptosis-protease activating factor 1 (Apaf-1) protein complex and the activation of caspase-9 (28). The Bcl-2 family is composed of proapoptotic and antiapoptotic members. The proapoptotic members Bax and Bak are crucial for the release of cytochrome *c* from mitochondria, by increasing the membrane permeability (30, 31).

As expected, HA-Bax coimmunoprecipitated with Flag-Bak and *vice versa* (Fig. 2A). Interestingly, endogenous Bax associated with Bak only upon SeV challenge in 293 cells, whereas Bax could not do so in the absence of SeV (Fig. 2B, left panel). Consistently, the same was true in MEF cells (Fig. 2B, right panel).

The antiapoptotic protein Bcl-2 promotes cell survival via binding to proapoptotic proteins. In resting cells, HA-Bax coimmunoprecipitated with Flag–Bcl-2 and *vice versa* (Fig. 2C). Notably, endogenous Bax dissociated from Bcl-2 upon SeV stimulation (Fig. 2D, left panel). This result was also confirmed in MEF cells (Fig. 2D, right panel). Furthermore, knockdown of endogenous Bax or Bak markedly attenuated the SeV-triggered cleavages of caspase-9 and PARP. In contrast, the cleavages of caspase-8 and PARP induced by TNF-α were not affected by depletion of either Bax or Bak (Fig. 2E). In addition, confocal imaging revealed that mitochondrial cytochrome *c* was released into the cytoplasm upon SeV infection (Fig. 2F). Taken together, these observations demonstrate that Sendai virus activates the intrinsic mitochondrial apoptosis pathway through proapoptotic Bak and Bax.

MAVS, Tom70, and IRF3 mediate SeV-induced apoptosis. MAVS, also named VISA, IPS-1, and CARDIF, localizes on the outer membrane of mitochondria through its C-terminal transmembrane domain (20–23). MAVS is important for activating type I interferon expression in innate immune signaling. Several recent studies demonstrated that MAVS also modulates virus-induced apoptosis (32, 33). We confirmed that SeV-induced apoptosis was markedly impaired in *mavs*$^{-/-}$ MEF cells (Fig. 3A, left panel). In contrast, TNF-α-induced apoptosis was not affected in *mavs*$^{-/-}$ MEF cells (Fig. 3A, right panel). MAVS could be cleaved at Cys-508 and was inactivated by NS3/4A, a serine protease from hepatitis C virus (34). Consistently, ectopic expression of NS3/4A attenuated the SeV-triggered cleavages of PARP and caspase-9 (Fig. 3B).

Recently, we characterized Tom70 as a critical adaptor for MAVS-mediated antiviral signaling (24). We speculated about whether Tom70 could modulate SeV-induced apoptosis. In exploring this possibility, we observed that ectopic expression of Tom70 augmented the SeV-triggered cleavage of PARP (Fig. 3C). In contrast, knocking down endogenous Tom70 attenuated the cleavages of caspase-9 and PARP (Fig. 3D, left panel). However, the cleavages of caspase-8 and PARP induced by TNF-α were not affected by depletion of endogenous Tom70 (Fig. 3D, right panel). Annexin V staining confirmed that silencing of Tom70 dampened cell apoptosis upon SeV infection (Fig. 3E). As a control, knockdown of endogenous Tom20 did not influence the cleavages of caspase-9 and PARP triggered by SeV stimulation (Fig. 3F).

To rule out the potential off-target effects of the Tom70 siRNA, an RNAi-resistant Tom70 construct (rTom70) was generated, in which silent mutations were introduced into the sequence targeted by the siRNA without changing the amino acid sequence of Tom70. The host cells were first transfected with the negative-control or Tom70 siRNA, followed by transfection with a control or rTom70 plasmid, respectively. The cleavages of caspase-9 and PARP were restored by introducing rTom70 into Tom70-knockdown cells (see Fig. 5F). These data indicate that Tom70 potentiates SeV-induced apoptosis.

Both Hiscott et al. and Sen et al. reported that IRF3 is indispensable for SeV-induced apoptosis (25, 35), and we confirmed this claim (Fig. 3G, left panel). In addition, the absence of IRF3 did not affect the cleavages of caspase-8 and PARP induced by TNF-α (Fig. 3G, right panel). Taken together, the data show that MAVS, Tom70, and IRF3 are indispensable for SeV-induced apoptosis.

Inhibition of Hsp90 or IKK-i impairs SeV-induced apoptosis. We recently reported that Hsp90 constitutively forms a complex with TBK1 and IRF3 in innate immune signaling (36). We wondered whether Hsp90 was essential for SeV-induced apoptosis. Radicicol (RA) and geldanamycin (GA) are small-molecule compounds that specifically bind to the ATP/ADP binding pocket of Hsp90 and inhibit the interaction between Hsp90 and its client proteins (37, 38). Notably, either GA or RA significantly impaired the cleavages of PARP and caspase-9 triggered by SeV (Fig. 4A and B, left panels). In contrast, neither GA nor RA influenced the cleavages of PARP and caspase-8 triggered by TNF-α (Fig. 4A and B, right panels). Furthermore, dimethyl sulfoxide (DMSO) displayed no effect on SeV-induced apoptosis or TNF-α-induced apoptosis (Fig. 4A and B).

To further substantiate this observation, knockdown of Hsp90 apparently reduced the SeV-induced cleavages of caspase-9 and PARP, whereas this did not affect the cleavages of caspase-8 and PARP triggered by TNF-α (Fig. 4C). To rule out the potential off-target effects of the Hsp90 siRNA, an RNAi-resistant Hsp90 construct (rHsp90) was generated, in which silent mutations were introduced into the sequence targeted by the siRNA without changing the amino acid sequence of Hsp90. The cells were first transfected with the negative-control or Hsp90 siRNA, followed by transfection with a control or rHsp90 plasmid, respectively. The cleavages of caspase-9 and PARP were restored by introducing rHsp90 into the endogenous Hsp90-silenced cells (see Fig. 5H). These results indicate that Hsp90 plays a positive role in SeV-induced apoptosis.

FIG 4 Inhibition of Hsp90 or IKK-i impairs Sendai virus-induced apoptosis. (A and B) HEK293 cells were treated with DMSO, RA (2.5 μM) (A), or GA (2 μM) (B) and then infected with SeV (left) or treated with TNF-α (10 ng/ml) and CHX (10 ng/ml) (right) for the indicated times. Cell lysates were collected and subjected to immunoblot analysis with the indicated antibodies. (C) HEK293 cells were transfected with NC or Hsp90 siRNA and then infected with SeV (left) or treated with TNF-α (10 ng/ml) and CHX (10 ng/ml) (right) for the indicated times. Cell lysates were collected for Western blot analysis with the indicated antibodies. (D) HEK293 cells were treated with BX795 (2.5 μM) or DMSO and infected with SeV (left) or treated with TNF-α (10 ng/ml) plus CHX (10 ng/ml) (right) for the indicated times. Cell lysates were collected and subjected to immunoblot analysis with the indicated antibodies. (E) HEK293 cells were transfected with the indicated siRNAs and then infected with SeV (left) or treated with TNF-α (10 ng/ml) and CHX (10 ng/ml) (right) for the indicated times. Cell lysates were collected for Western blot analysis with the indicated antibodies. NC, negative-control siRNA; *, nonspecific band.

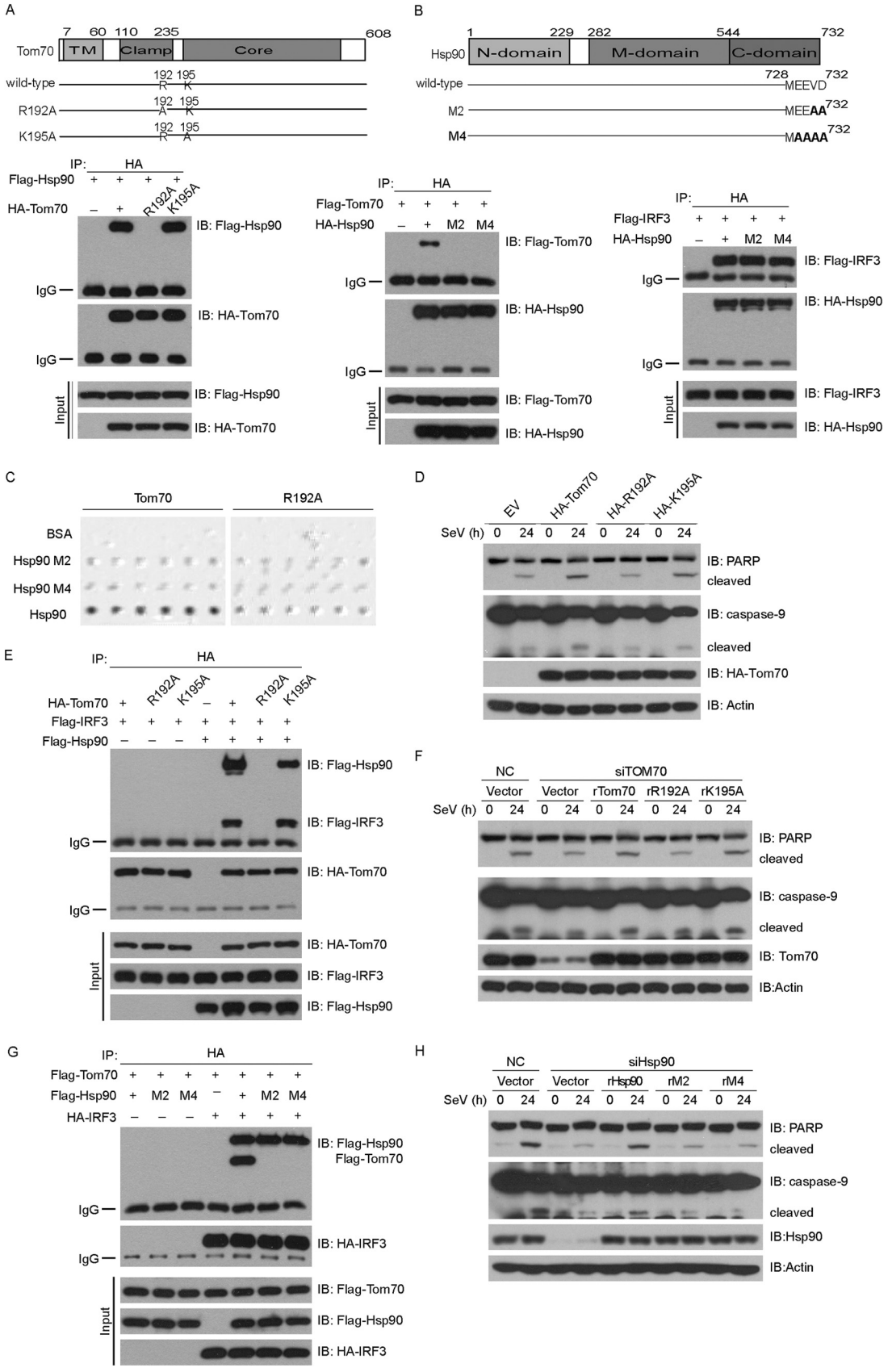
A
7 60 110 235 608
Tom70 TM Clamp Core
wild-type 192 R 195 K
R192A 192 A 195 K
K195A 192 R 195 A
B
1 229 282 544 732
Hsp90 N-domain M-domain C-domain
wild-type 728 MEEVD 732
M2 MEEAA 732
M4 MAAAA 732
IP: HA
Flag-Hsp90 + + + +
HA-Tom70 – + R192A K195A
IB: Flag-Hsp90
IgG
IB: HA-Tom70
IgG
Input
IB: Flag-Hsp90
IB: HA-Tom70
IP: HA
Flag-Tom70 + + + +
HA-Hsp90 – + M2 M4
IB: Flag-Tom70
IgG
IB: HA-Hsp90
IgG
Input
IB: Flag-Tom70
IB: HA-Hsp90
IP: HA
Flag-IRF3 + + + +
HA-Hsp90 – + M2 M4
IB: Flag-IRF3
IgG
IB: HA-Hsp90
IgG
Input
IB: Flag-IRF3
IB: HA-Hsp90
C
Tom70 R192A
BSA
Hsp90 M2
Hsp90 M4
Hsp90
D
EV HA-Tom70 HA-R192A HA-K195A
SeV (h) 0 24 0 24 0 24 0 24
IB: PARP
cleaved
IB: caspase-9
cleaved
IB: HA-Tom70
IB: Actin
E
IP: HA
HA-Tom70 + R192A K195A – + R192A K195A
Flag-IRF3 + + + + + + +
Flag-Hsp90 – – – + + + +
IB: Flag-Hsp90
IB: Flag-IRF3
IgG
IB: HA-Tom70
IgG
Input
IB: HA-Tom70
IB: Flag-IRF3
IB: Flag-Hsp90
F
NC siTOM70
Vector Vector rTom70 rR192A rK195A
SeV (h) 0 24 0 24 0 24 0 24 0 24
IB: PARP
cleaved
IB: caspase-9
cleaved
IB: Tom70
IB:Actin
G
IP: HA
Flag-Tom70 + + + + + + +
Flag-Hsp90 + M2 M4 – + M2 M4
HA-IRF3 – – – + + + +
IB: Flag-Hsp90
Flag-Tom70
IgG
IB: HA-IRF3
IgG
Input
IB: Flag-Tom70
IB: Flag-Hsp90
IB: HA-IRF3
H
NC siHsp90
Vector Vector rHsp90 rM2 rM4
SeV (h) 0 24 0 24 0 24 0 24 0 24
IB: PARP
cleaved
IB: caspase-9
cleaved
IB:Hsp90
IB:Actin

As an antagonist effective against both IKK-i and TBK1, BX795 has been used to block the activation of IRF3 induced by SeV (39). Interestingly, BX795 also impaired the cleavages of caspase-9 and PARP triggered by SeV, whereas it had no effects on the cleavages of caspase-8 and PARP triggered by TNF-α (Fig. 4D). To our surprise, depletion of endogenous IKK-i, but not TBK1, significantly impaired SeV-induced apoptosis (Fig. 4E, left panel). However, knocking down either IKK-i or TBK1 had no impact on TNF-α-induced apoptosis (Fig. 4E, right panel). These observations suggest that TBK1 and IKK-i play nonredundant functions in innate immune signaling and apoptosis, respectively.

Tom70, Hsp90, and IRF3 form a dynamic complex in SeV-induced apoptosis. The chaperone Hsp90 was reported to interact dynamically with the mitochondrial outer membrane protein Tom70 (19). We wondered whether the Tom70/Hsp90/IRF3 protein complex is critical for SeV-induced apoptosis, so we generated two Tom70 point mutants, Tom70 (R192A) and Tom70 (K195A), which are mutated in the clamp domain of Tom70. As expected, ectopically expressed Hsp90 could bind to Tom70 (Fig. 5A). Notably, Tom70 (R192A) could not interact with Hsp90, but Tom70 (K195A) still interacted with Hsp90 (Fig. 5A and E). The Hsp90 N-terminal domain (amino acids 1 to 232) was both necessary and sufficient to specifically interact with IRF3 (36), whereas the C-terminal EEVD motif of Hsp90 mediated its binding to Tom70. Therefore, the EEVD motif of Hsp90 was mutated to EEAA [Hsp90 (M2)] or AAAA [Hsp90 (M4)] (Fig. 5B). As shown in Fig. 5B, Hsp90 (M2) and Hsp90 (M4) could not interact with Tom70 (left panel), while these mutants could still interact with IRF3 (right panel).

We investigated the interaction between Tom70 and Hsp90 via the oblique-incidence reflectivity difference (OIRD) method (27). We observed that Tom70 interacted directly with Hsp90, whereas Tom70 (R192A), Hsp90 (M2), or Hsp90 (M4) failed to mediate this direct interaction (Fig. 5C). Due to the technical limitations, we were not able to collect interaction data for the Tom70/Hsp90/IRF3 protein complex.

Consistently, in contrast to the case with the wild type, ectopic expression of Tom70 (R192A) could not augment the cleavages of caspase-9 and PARP, whereas that of Tom70 (K195A) could markedly potentiate this process (Fig. 5D). Tom70 interacted with IRF3 via Hsp90, so IRF3 failed to associate with Tom70 (R192A), whereas it could still associate with Tom70 (K195A) (Fig. 5E). Furthermore, we generated the corresponding RNAi-resistant constructs of Tom70 (R192A) and Tom70 (K195A), namely, rTom70 (rR192A) and rTom70 (rK195A). Consistently, only rTom70 (rK195A) could rescue the cleavages of caspase-9 and PARP after the endogenous Tom70 was depleted, as well as the wild-type rTom70. In contrast, rTom70 (rR192A) failed to restore the cleavages of caspase-9 and PARP (Fig. 5F).

The wild-type and mutant forms of Hsp90 were ectopically expressed with Tom70 and IRF3 in different combinations and then subjected to a coimmunoprecipitation assay. As shown in Fig. 5G, IRF3 could interact with Tom70 via wild-type Hsp90 but not via Hsp90 (M2) and Hsp90 (M4). We then generated RNAi-resistant Hsp90 mutants in the backgrounds of Hsp90 (M2) and Hsp90 (M4) and named them rHsp90 (M2) and rHsp90 (M4), respectively. We observed that neither rHsp90 (M2) nor rHsp90 (M4) could restore the cleavages of caspase-9 and PARP in Hsp90-knockdown cells (Fig. 5H). Collectively, these data demonstrate that formation of the Tom70/Hsp90/IRF3 complex is necessary for SeV-induced apoptosis.

IRF3 is recruited to mitochondria via Tom70/Hsp90 in SeV-induced apoptosis. Tom70 resides on the outer membrane of mitochondria, whereas IRF3 is located in the cytosol of resting cells. We investigated whether Tom70 could dynamically recruit IRF3 to mitochondria upon virus infection. Subcellular fractionation methods revealed that both ectopically expressed IRF3 (Fig. 6A) and endogenous IRF3 (Fig. 6B) relocalized to mitochondria upon SeV stimulation. It was observed that SeV stimulation resulted in a phosphorylated form of IRF3 (form II) (40). Notably, extended SeV infection induced the ubiquitin-proteasome-mediated degradation of IRF3 (Fig. 6C).

We next examined the effect of the Tom70 knockdown on the recruitment of IRF3 to mitochondria that was triggered by SeV. Depletion of endogenous Tom70 by use of siRNA dramatically inhibited the recruitment of IRF3 to mitochondria (Fig. 6D). As a negative control, knockdown of endogenous Tom20 displayed no effect on the cytoplasm-to-mitochondrion translocation of IRF3 (Fig. 6E). These results were consistent with the above observation that Tom70 knockdown dramatically inhibited SeV-induced apoptosis, whereas knockdown of Tom20 failed to do so (Fig. 3F).

To rule out the potential off-target effect of Tom70 siRNA, rescue experiments were carried out. The host cells were first transfected with nonspecific or Tom70 siRNA, followed by transfection with a control or RNAi-resistant Tom70 plasmid, respectively. As shown in Fig. 6F, the SeV-induced cytoplasm-to-mitochondrion translocation of IRF3 was restored only by introducing rTom70 into the Tom70-knockdown cells, whereas rTom70 (rR192A) failed to restore this function. These observations were consistent with the observation that rTom70 rescued the cleavages of caspase-9 and PARP, whereas rTom70 (rR192A) did not have such rescue effects. Collectively, these data indicate that Tom70/Hsp90 recruits the cytoplasmic IRF3 protein to mitochondria to mediate SeV-induced apoptosis.

SeV induces the formation of a novel apoptosis complex (Tom70/Hsp90/IRF3/Bax). The proapoptotic protein Bax and the antiapoptotic protein Bcl-2 are key regulators of the intrinsic apoptosis pathway (28). Bcl-2 is a membrane-associated protein on the mitochondrial outer membrane, whereas Bax resides in the

FIG 5 Tom70, Hsp90, and IRF3 form a dynamic complex during Sendai virus-induced apoptosis. (A, B, E, and G) HEK293T cells were transfected with the indicated constructs for 36 h and then subjected to immunoprecipitation with anti-HA antibody. The immunoprecipitates were analyzed by immunoblotting with the indicated antibodies. TM, transmembrane domain. (C) The interactions between Tom70 and Hsp90 were tested by the oblique-incidence reflectivity difference method. (D) HEK293 cells were transfected with the indicated plasmids for 24 h and then infected with SeV for the indicated times. Cell lysates were analyzed by immunoblotting with the indicated antibodies. (F) HEK293 cells were first transfected with NC or Tom70 siRNA and then rescued with the indicated siRNA-resistant Tom70 constructs. Cell lysates were collected for Western blot analysis with the indicated antibodies. (H) HEK293 cells were first transfected with NC or Hsp90 siRNA and then rescued with the indicated siRNA-resistant Hsp90 constructs. Cell lysates were collected for Western blot analysis with the indicated antibodies. NC, nonspecific control siRNA; R192A, K195A, rTom70, rR192A, and rK195A, point mutants of Tom70; M2, M4, rHsp90, rM2, and rM4, point mutants of Hsp90.

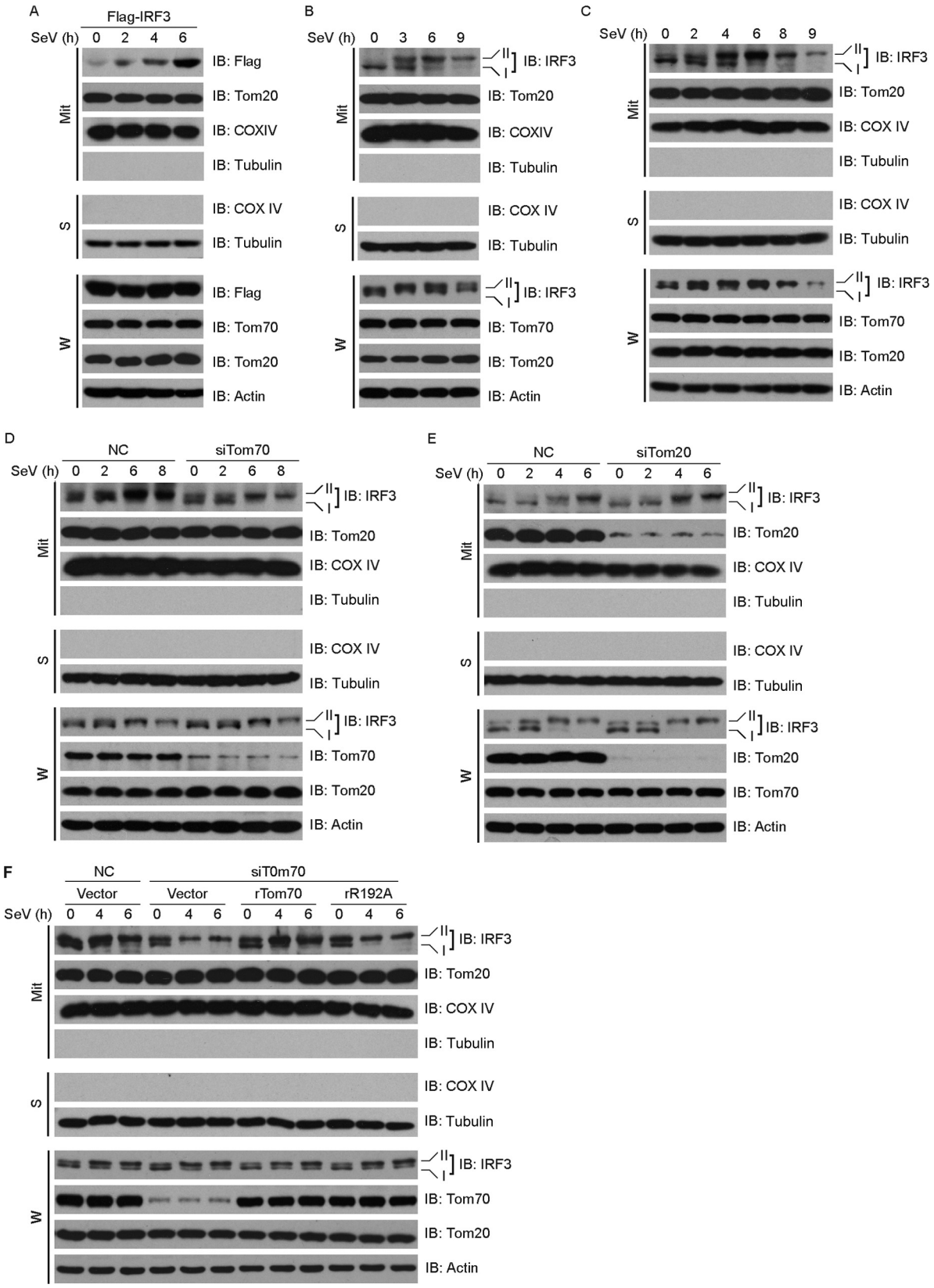

FIG 6 IRF3 is recruited to mitochondria via Tom70/Hsp90 during Sendai virus-induced apoptosis. (A) Flag-IRF3 was ectopically expressed in HEK293 cells, which were then stimulated with SeV for the indicated times. Lysates of whole cells (W) and of mitochondria isolated from the virus-infected cells (Mit) were immunoblotted with the indicated antibodies. (B and C) HEK293 cells were challenged by SeV infection for the indicated times, and then lysates of the whole cells (W) and of mitochondria isolated from the virus-infected cells (Mit) were immunoblotted with the indicated antibodies. (D and E) HEK293 cells were transfected

cytosol and translocates onto the mitochondrial membrane upon apoptotic stimulation (30).

We wondered whether Bcl-2 or Bax could interact with the Tom70/Hsp90/IRF3 complex upon SeV infection. Interestingly, Flag-IRF3 coimmunoprecipitated with HA–Bcl-2 (Fig. 7A, left panel). Consistently, endogenous IRF3 associated with endogenous Bcl-2 in resting cells. Note that this interaction decreased markedly upon SeV stimulation (Fig. 7A, right panel). Flag-IRF3 could also be coimmunoprecipitated with HA-Bax (Fig. 7B, left panel). In contrast, IRF3 marginally interacted with endogenous Bax in resting cells (Fig. 7B, left panel). However, the interaction between IRF3 and Bax was greatly enhanced upon SeV challenge (Fig. 7B, left panel). These data indicate that IRF3 dynamically interacts with Bcl-2 or Bax in different cell states.

To dissect the relationship among Tom70, Hsp90, IRF3, and Bax, different combinations of these proteins were ectopically expressed in HEK293T cells. The coimmunoprecipitation assays revealed that Bax interacted directly with IRF3 but not with Hsp90 or Tom70 (Fig. 7C, left panel). This was also confirmed endogenously (Fig. 7C, right panel). Thus, SeV induces the formation of the Tom70/Hsp90/IRF3/Bax protein complex, which represents a novel apoptosis signalosome on the mitochondrial outer membrane.

We wondered whether the SeV-induced mitochondrial translocation of Bax was dependent on IRF3 or Tom70. To address this possibility, we isolated mitochondria to probe the distribution of Bax upon SeV infection. Significantly more Bax was present on mitochondria upon SeV stimulation, and this was directly related to the duration of the infection (Fig. 7D). Note that silencing of endogenous Tom70 by use of siRNA dramatically impaired the translation of Bax onto mitochondria that was triggered by SeV (Fig. 7E). In addition, we observed that the SeV-triggered mitochondrial translocation of Bax was abolished in *irf3*$^{-/-}$ MEF cells (Fig. 7F). These results suggested that relocation of Bax was dependent on the Tom70/IRF3 complex.

On mitochondria, Bax could associate with Bcl-2 (antiapoptotic) or Bak (proapoptotic), thus switching the fate (survival or apoptosis) of host cells. We observed that depletion of Tom70 promoted the association of the Bax and Bcl-2 complex, attenuating the dissociation of Bax from Bcl-2 triggered by SeV (Fig. 7G, upper panels). In contrast, silencing of Tom20 had no influence on the stability or dissociation of the Bax and Bcl-2 complex (Fig. 7G, lower panels). Furthermore, confocal imaging demonstrated that depletion of Tom70 attenuated the release of cytochrome *c* from mitochondria to the cytosol (Fig. 7H).

DISCUSSION

RIG-I-like receptors and Toll-like receptors detect viruses from topologically intracellular and extracellular compartments and initiate the immediate innate immunity, representing the first line of host defenses to restrict virus infection and proliferation. In the meantime, infected cells are prone to apoptosis to restrain the spread of virus. IRF3 was first characterized as a key transcription factor for inducing the expression of type I interferons and inflammatory cytokines upon stimulation by various stimuli, such as double-stranded RNA (dsRNA), CpG DNA, and lipopolysaccharide (LPS).

Unexpectedly, Hiscott et al. demonstrated that SeV-induced apoptosis was also dependent on IRF3, but its transcriptional activity was dispensable for the induction of apoptosis (25). Ting et al. reported that MAVS$^{-/-}$ fibroblasts were resistant to SeV-induced apoptosis (32). These investigations indicate that SeV may induce partially overlapping signaling pathways to mediate innate immunity and apoptosis. However, the specific molecular mechanism of SeV-induced apoptosis remains to be characterized.

In this study, we confirmed that MAVS promotes SeV-induced apoptosis and that its mitochondrial localization is necessary for this function (Fig. 3A and B). In addition, we discovered that Tom70 is important for SeV-induced apoptosis. Several lines of evidence substantiate the claim that Tom70 recruits IRF3 to mitochondria via Hsp90. First, antagonists of Hsp90 (RA and GA), which inhibit its ATPase activity, impaired SeV-induced apoptosis but did not affect TNF-α-induced apoptosis (Fig. 4A and B). Second, depletion of endogenous Tom70 or Hsp90 markedly impaired SeV-induced apoptosis but did not affect TNF-α-induced apoptosis (Fig. 3D and E and 4C). This attenuation could be rescued by exogenously expressing siRNA-resistant rTom70 or rHsp90. Third, the Tom70 (R192A) mutant, which could not interact with Hsp90, inhibited SeV-induced apoptosis, whereas the Tom70 (K195A) mutant, which could interact with Hsp90, promoted SeV-induced apoptosis. The RNAi-resistant mutant(s) of Tom70 (R192A) [rTom70 (rR192A)] or Hsp90 (rM2 and rM4) failed to rescue SeV-induced apoptosis when endogenous Tom70 or Hsp90, respectively, was knocked down (Fig. 5F and H). In contrast, the rTom70 (rK195A) mutant could rescue this effect. Fourth, Tom70, Hsp90, and IRF3 formed a dynamic protein complex endogenously (Fig. 7C). Fifth, IRF3 was translocated from the cytoplasm onto mitochondria upon SeV challenge, and this was dependent on Tom70 and Hsp90 (Fig. 6).

In normal cells, proapoptotic Bak and Bax are kept in check by a prosurvival protein, for example, Bcl-2. Interestingly, our current study revealed that IRF3 specifically associates with Bax (Fig. 7B) and promotes the dissociation of Bax from Bcl-2 upon SeV stimulation (Fig. 2D). We demonstrated that cytosolic Bax was translocated onto mitochondria during SeV-induced apoptosis and that SeV triggered Tom70, Hsp90, IRF3, and Bax to form a novel complex on mitochondria. Depletion of Tom70 and IRF3 drastically abolished the translocation of Bax (Fig. 7C to F). Chattopadhyay et al. also reported the IRF3-mediated Bax activation and translocation to mitochondria (41). Based on the current insights, the following tentative model is proposed: Tom70 recruits the cytosolic Hsp90/IRF3/Bax complex to the mitochondrial outer membrane upon SeV stimulation (Fig. 8), which facilitates the formation of the Bax and Bak channel, thus promoting the release of cytochrome *c*.

Young et al. recently reported that the dissociation constant

with NC siRNA, Tom70 siRNA (D), or Tom20 siRNA (E) for 48 h and then stimulated with SeV for the indicated times. Lysates of whole cells (W) and of mitochondria (Mit) were resolved by SDS-PAGE and then immunoblotted with the indicated antibodies. (F) HEK293 cells were transfected with control or Tom70 siRNA and then rescued with the indicated siRNA-resistant Tom70 constructs. The cells were fractionated, and the whole-cell lysates (W) and lysates of mitochondria (Mit) were immunoblotted with the indicated antibodies. NC, negative control; rTom70 and rR192A, point mutants of Tom70; W, whole-cell lysates; Mit, lysates of mitochondrial fraction; S, cytosolic part.

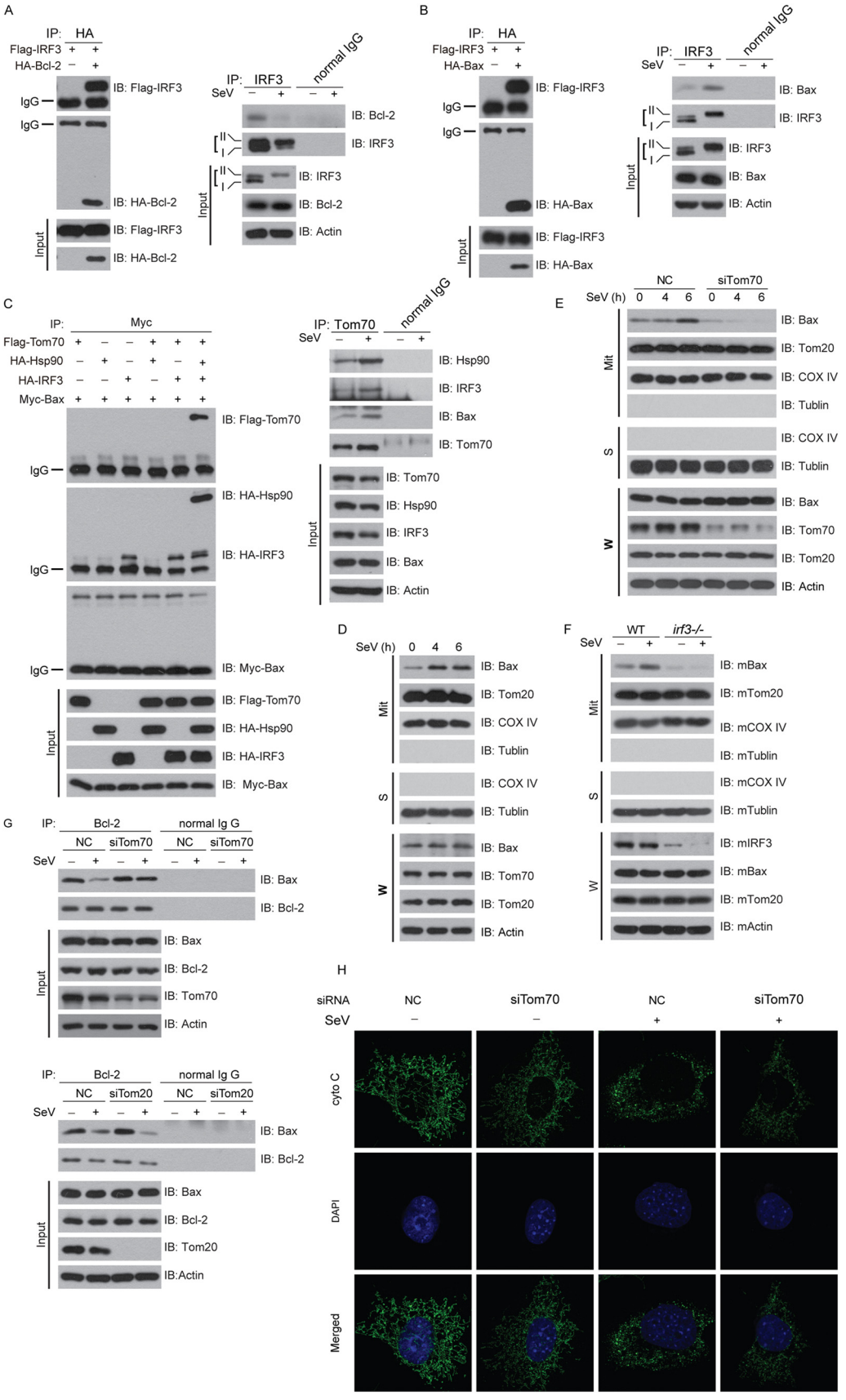
A
IP: HA
Flag-IRF3 + +
HA-Bcl-2 – +
IB: Flag-IRF3
IgG
IgG
IB: HA-Bcl-2
Input
IB: Flag-IRF3
IB: HA-Bcl-2
IP: IRF3
normal IgG
SeV – + – +
IB: Bcl-2
IB: IRF3
Input
IB: IRF3
IB: Bcl-2
IB: Actin
B
IP: HA
Flag-IRF3 + +
HA-Bax – +
IB: Flag-IRF3
IgG
IgG
IB: HA-Bax
Input
IB: Flag-IRF3
IB: HA-Bax
IP: IRF3
normal IgG
SeV – + – +
IB: Bax
IB: IRF3
Input
IB: IRF3
IB: Bax
IB: Actin
C
IP: Myc
Flag-Tom70 + – – + + +
HA-Hsp90 – + – + – +
HA-IRF3 – – + – + +
Myc-Bax + + + + + +
IB: Flag-Tom70
IgG
IB: HA-Hsp90
IgG
IB: HA-IRF3
IgG
IB: Myc-Bax
Input
IB: Flag-Tom70
IB: HA-Hsp90
IB: HA-IRF3
IB: Myc-Bax
IP: Tom70
normal IgG
SeV – + – +
IB: Hsp90
IB: IRF3
IB: Bax
IB: Tom70
Input
IB: Tom70
IB: Hsp90
IB: IRF3
IB: Bax
IB: Actin
D
SeV (h) 0 4 6
Mit
IB: Bax
IB: Tom20
IB: COX IV
IB: Tublin
S
IB: COX IV
IB: Tublin
W
IB: Bax
IB: Tom70
IB: Tom20
IB: Actin
E
NC siTom70
SeV (h) 0 4 6 0 4 6
Mit
IB: Bax
IB: Tom20
IB: COX IV
IB: Tublin
S
IB: COX IV
IB: Tublin
W
IB: Bax
IB: Tom70
IB: Tom20
IB: Actin
F
WT irf3-/-
SeV – + – +
Mit
IB: mBax
IB: mTom20
IB: mCOX IV
IB: mTublin
S
IB: mCOX IV
IB: mTublin
W
IB: mIRF3
IB: mBax
IB: mTom20
IB: mActin
G
IP: Bcl-2
normal Ig G
NC siTom70 NC siTom70
SeV – + – + – + – +
IB: Bax
IB: Bcl-2
Input
IB: Bax
IB: Bcl-2
IB: Tom70
IB: Actin
IP: Bcl-2
normal Ig G
NC siTom20 NC siTom20
SeV – + – + – + – +
IB: Bax
IB: Bcl-2
Input
IB: Bax
IB: Bcl-2
IB: Tom20
IB:Actin
H
siRNA NC siTom70 NC siTom70
SeV – – + +
cyto C
DAPI
Merged

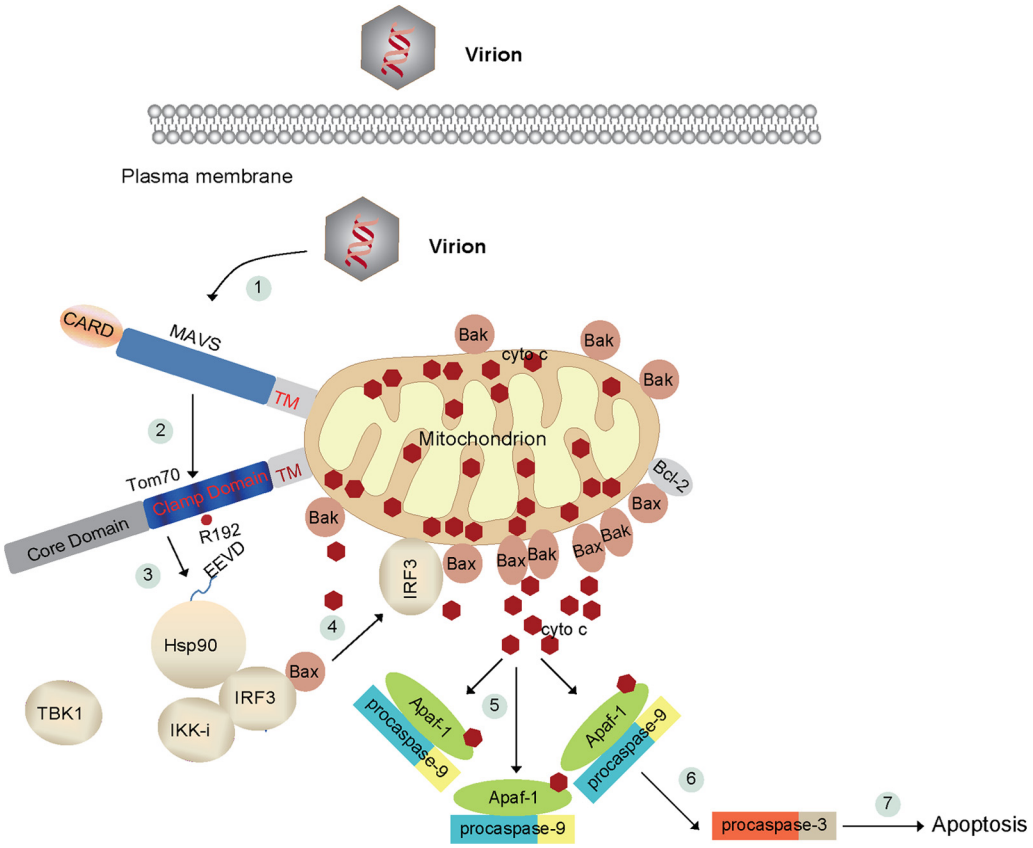

FIG 8 Schematic diagram of SeV-induced apoptosis. In resting cells, cytochrome *c* localizes to the mitochondrial intermembrane spaces, whereas Hsp90, IRF3, and Bax form a dynamic complex in the cytoplasm. (1) SeV triggers activation of the adapter MAVS on the outer membrane of mitochondria. (2) MAVS then associates with Tom70 via their transmembrane domains. (3) In the meantime, Hsp90 delivers IRF3/Bax onto the mitochondrial outer membrane via the clamp domain of Tom70 and the EEVD motif of Hsp90. Mitochondrial Bax dynamically interacts with Bak or Bcl-2. (4) Bax and Bak increase the permeability of the mitochondrial outer membrane, which results in the release of cytochrome *c* into the cytosol. The cytosolic cytochrome *c* binds to Apaf-1 and pro-caspase-9 (5) and activates pro-caspase-9 (6). Caspase-9 cleaves and activates the downstream executioner caspases, such as caspase-3. Ultimately, caspase-3 triggers the apoptotic responses. (7) For example, PARP is cleaved and inactivated by caspase-3.

(K_d) of the Hsp90-Tom70 interaction is 1.14 μM (42). We preliminarily calculated the K_d of Tom70-Hsp90, via the OIRD method, to be 54 nM, which is much smaller than 1.14 μM. The difference may be due to the different methods of measurement. It is technically difficult to investigate the direct interaction among the proteins of the Tom70/Hsp90/IRF3/Bax complex via the biophysical approach.

Both TBK1 and IKK-i could phosphorylate IRF3. Biochemical and genetic studies have well established that TBK1 is essential for activating innate immune signaling, whereas IKK-i is dispensable for innate immune signaling (43). Unexpectedly, our current study uncovered that IKK-i is essential for SeV-induced apoptosis, whereas TBK1 is dispensable for this apoptosis, revealing the nonredundant functions of TBK1 and IKK-i. Previous studies indicated that both IKK-i and TBK1 can phosphorylate the C-terminal activation domain of IRF3. It remains to be addressed how IKK-i modulates SeV-induced apoptosis. Recently, IRF3 was reported to mediate alcoholic liver disease via linking endoplasmic

FIG 7 Sendai virus induces formation of a novel apoptosis complex (Tom70/Hsp90/IRF3/Bax). (A and B) (Left) HEK293T cells were transfected with the indicated plasmids for 36 h and then subjected to immunoprecipitation with anti-HA antibody. (Right) HEK293 cells were stimulated with SeV for 24 h, and then cell lysates were subjected to immunoprecipitation with anti-IRF3 antibody or normal IgG. The immunoprecipitates were analyzed by immunoblotting with the indicated antibodies. (C) (Left) HEK293T cells were transfected with the indicated plasmids for 36 h and then subjected to immunoprecipitation with anti-MYC antibody. (Right) HEK293 cells were stimulated with SeV for 24 h, and then cell lysates were subjected to immunoprecipitation with anti-Tom70 antibody or normal IgG. The immunoprecipitates were analyzed by immunoblotting with the indicated antibodies. (D) HEK293 cells were challenged by SeV infection for the indicated times, and then lysates of whole cells (W) and of mitochondria isolated from the virus-infected cells (Mit) were immunoblotted with the indicated antibodies. (E) HEK293 cells were transfected with NC or Tom70 siRNA and then challenged with SeV for the indicated times. Lysates of whole cells (W) and of mitochondria (Mit) were resolved by SDS-PAGE and then immunoblotted with the indicated antibodies. (F) *irf3*$^{-/-}$ cells were infected with SeV for the indicated times. Lysates of whole cells (W) and of mitochondria (Mit) were resolved by SDS-PAGE and then immunoblotted with the indicated antibodies. (G) HEK293 cells were transfected with NC siRNA, Tom70 siRNA (upper panel), or Tom20 siRNA (lower panel) and then stimulated with SeV for 24 h, and then cell lysates were subjected to immunoprecipitation with anti-Bcl-2 antibody or normal IgG. (H) MEF cells were transfected with NC or Tom70 siRNA and then infected with SeV. Cells were stained with anti-cytochrome *c* antibody and then imaged by confocal microscopy. NC, negative control; W, whole-cell lysates; Mit, lysates of mitochondrial fraction; S, cytosolic part.

reticulum (ER) stress with apoptotic signaling in hepatocytes, independently of inflammatory cytokines and IFNs (44). MiniMAVS was recently identified as an N-terminally truncated variant of full-length MAVS which also resides on mitochondria. MiniMAVS interfered with production of interferon induced by full-length MAVS, but it also positively regulated cell death (45). It is suggested that the N-terminal CARD and PRR domains of MAVS are dispensable for virus-induced apoptosis but essential for interferon production. We speculate that MAVS and IRF3 may broadly modulate apoptosis in other systems, such as development and cancer, but this requires further investigation.

ACKNOWLEDGMENTS

We thank Mian Wu (University of Science and Technology of China) and Jian-Sheng Kang (Shanghai Institute of Nutrition, Chinese Academy of Science) for providing plasmids for this study. We thank Michael Holt (National Institutes of Health) for kindly editing the manuscript.

C.W. was supported by grants from the National Natural Science Foundation of China (grants 31030021 and 81161120542) and the Ministry of Science and Technology of China (grants 2012CB910200 and 2011CB910904). Q.Z. was funded by the National Basic Research Program of China (grant 2011CB944002) and the National Natural Science Foundation of China (grant 31271563).

We have no financial conflicts of interest.

REFERENCES

1. **Meylan E, Tschopp J.** 2006. Toll-like receptors and RNA helicases: two parallel ways to trigger antiviral responses. Mol Cell **22:**561–569. http://dx.doi.org/10.1016/j.molcel.2006.05.012.
2. **Sun LJ, Wu JX, Du FH, Chen X, Chen ZJJ.** 2013. Cyclic GMP-AMP synthase is a cytosolic DNA sensor that activates the type I interferon pathway. Science **339:**786–791. http://dx.doi.org/10.1126/science.1232458.
3. **Akira S, Uematsu S, Takeuchi O.** 2006. Pathogen recognition and innate immunity. Cell **124:**783–801. http://dx.doi.org/10.1016/j.cell.2006.02.015.
4. **Green DR, Reed JC.** 1998. Mitochondria and apoptosis. Science **281:**1309–1312. http://dx.doi.org/10.1126/science.281.5381.1309.
5. **Carson DA, Ribeiro JM.** 1993. Apoptosis and disease. Lancet **341:**1251–1254. http://dx.doi.org/10.1016/0140-6736(93)91154-E.
6. **Lenardo M, Chan FKM, Hornung F, McFarland H, Siegel R, Wang J, Zheng LX.** 1999. Mature T lymphocyte apoptosis—immune regulation in a dynamic and unpredictable antigenic environment. Annu Rev Immunol **17:**221–253. http://dx.doi.org/10.1146/annurev.immunol.17.1.221.
7. **Lettre G, Hengartner MO.** 2006. Developmental apoptosis in C-elegans: a complex CEDnario. Nat Rev Mol Cell Biol **7:**97–108. http://dx.doi.org/10.1038/nrm1836.
8. **Yuan JY, Yankner BA.** 2000. Apoptosis in the nervous system. Nature **407:**802–809. http://dx.doi.org/10.1038/35037739.
9. **Zitvogel L, Kepp O, Kroemer G.** 2010. Decoding cell death signals in inflammation and immunity. Cell **140:**798–804. http://dx.doi.org/10.1016/j.cell.2010.02.015.
10. **Schultz-Cherry S, Dybdahl-Sissoko N, Neumann G, Kawaoka Y, Hinshaw VS.** 2001. Influenza virus NS1 protein induces apoptosis in cultured cells. J Virol **75:**7875–7881. http://dx.doi.org/10.1128/JVI.75.17.7875-7881.2001.
11. **Zhirnov OP, Konakova TE, Wolff T, Klenk HD.** 2002. NS1 protein of influenza A virus down-regulates apoptosis. J Virol **76:**1617–1625. http://dx.doi.org/10.1128/JVI.76.4.1617-1625.2002.
12. **Gil J, Alcami J, Esteban M.** 1999. Induction of apoptosis by double-stranded-RNA-dependent protein kinase (PKR) involves the alpha subunit of eukaryotic translation initiation factor 2 and NF-kappaB. Mol Cell Biol **19:**4653–4663.
13. **Cheng EH, Nicholas J, Bellows DS, Hayward GS, Guo HG, Reitz MS, Hardwick JM.** 1997. A Bcl-2 homolog encoded by Kaposi sarcoma-associated virus, human herpesvirus 8, inhibits apoptosis but does not heterodimerize with Bax or Bak. Proc Natl Acad Sci U S A **94:**690–694. http://dx.doi.org/10.1073/pnas.94.2.690.
14. **Lee JS, Li Q, Lee JY, Lee SH, Jeong JH, Lee HR, Chang H, Zhou FC, Gao SJ, Liang C, Jung JU.** 2009. FLIP-mediated autophagy regulation in cell death control. Nat Cell Biol **11:**1355–1362. http://dx.doi.org/10.1038/ncb1980.
15. **Neilan JG, Lu Z, Afonso CL, Kutish GF, Sussman MD, Rock DL.** 1993. An African swine fever virus gene with similarity to the proto-oncogene bcl-2 and the Epstein-Barr virus gene BHRF1. J Virol **67:**4391–4394.
16. **Neupert W, Herrmann JM.** 2007. Translocation of proteins into mitochondria. Annu Rev Biochem **76:**723–749. http://dx.doi.org/10.1146/annurev.biochem.76.052705.163409.
17. **Baker MJ, Frazier AE, Gulbis JM, Ryan MT.** 2007. Mitochondrial protein-import machinery: correlating structure with function. Trends Cell Biol **17:**456–464. http://dx.doi.org/10.1016/j.tcb.2007.07.010.
18. **Chacinska A, Koehler CM, Milenkovic D, Lithgow T, Pfanner N.** 2009. Importing mitochondrial proteins: machineries and mechanisms. Cell **138:**628–644. http://dx.doi.org/10.1016/j.cell.2009.08.005.
19. **Young JC, Hoogenraad NJ, Hartl FU.** 2003. Molecular chaperones Hsp90 and Hsp70 deliver preproteins to the mitochondrial import receptor Tom70. Cell **112:**41–50. http://dx.doi.org/10.1016/S0092-8674(02)01250-3.
20. **Kawai T, Takahashi K, Sato S, Coban C, Kumar H, Kato H, Ishii KJ, Takeuchi O, Akira S.** 2005. IPS-1, an adaptor triggering RIG-I- and Mda5-mediated type I interferon induction. Nat Immunol **6:**981–988. http://dx.doi.org/10.1038/ni1243.
21. **Meylan E, Curran J, Hofmann K, Moradpour D, Binder M, Bartenschlager R, Tschopp J.** 2005. Cardif is an adaptor protein in the RIG-I antiviral pathway and is targeted by hepatitis C virus. Nature **437:**1167–1172. http://dx.doi.org/10.1038/nature04193.
22. **Seth RB, Sun L, Ea CK, Chen ZJ.** 2005. Identification and characterization of MAVS, a mitochondrial antiviral signaling protein that activates NF-kappaB and IRF 3. Cell **122:**669–682. http://dx.doi.org/10.1016/j.cell.2005.08.012.
23. **Xu LG, Wang YY, Han KJ, Li LY, Zhai Z, Shu HB.** 2005. VISA is an adapter protein required for virus-triggered IFN-beta signaling. Mol Cell **19:**727–740. http://dx.doi.org/10.1016/j.molcel.2005.08.014.
24. **Liu XY, Wei B, Shi HX, Shan YF, Wang C.** 2010. Tom70 mediates activation of interferon regulatory factor 3 on mitochondria. Cell Res **20:**994–1011. http://dx.doi.org/10.1038/cr.2010.103.
25. **Heylbroeck C, Balachandran S, Servant MJ, DeLuca C, Barber GN, Lin R, Hiscott J.** 2000. The IRF-3 transcription factor mediates Sendai virus-induced apoptosis. J Virol **74:**3781–3792. http://dx.doi.org/10.1128/JVI.74.8.3781-3792.2000.
26. **Hu WH, Liu YS, Lu ZS, Li CM.** 2010. Poly[oligo(ethylene glycol) methacrylate-co-glycidyl methacrylate] brush substrate for sensitive surface plasmon resonance imaging protein arrays. Adv Funct Mater **20:**3497–3503. http://dx.doi.org/10.1002/adfm.201001159.
27. **Lu H, Wen JA, Wang X, Yuan K, Li W, Lu HB, Zhou YL, Jin KJ, Ruan KC, Yang GZ.** 2010. Detection of the specific binding on protein microarrays by oblique-incidence reflectivity difference method. J Optics **12:**095301. http://dx.doi.org/10.1088/2040-8978/12/9/095301.
28. **Hengartner MO.** 2000. The biochemistry of apoptosis. Nature **407:**770–776. http://dx.doi.org/10.1038/35037710.
29. **Oliver FJ, de la Rubia G, Rolli V, Ruiz-Ruiz MC, de Murcia G, Murcia JM.** 1998. Importance of poly(ADP-ribose) polymerase and its cleavage in apoptosis. Lesson from an uncleavable mutant. J Biol Chem **273:**33533–33539.
30. **Gross A, McDonnell JM, Korsmeyer SJ.** 1999. BCL-2 family members and the mitochondria in apoptosis. Genes Dev **13:**1899–1911. http://dx.doi.org/10.1101/gad.13.15.1899.
31. **Wei MC, Zong WX, Cheng EHY, Lindsten T, Panoutsakopoulou V, Ross AJ, Roth KA, MacGregor GR, Thompson CB, Korsmeyer SJ.** 2001. Proapoptotic BAX and BAK: a requisite gateway to mitochondrial dysfunction and death. Science **292:**727–730. http://dx.doi.org/10.1126/science.1059108.
32. **Lei Y, Moore CB, Liesman RM, O'Connor BP, Bergstralh DT, Chen ZJ, Pickles RJ, Ting JP.** 2009. MAVS-mediated apoptosis and its inhibition by viral proteins. PLoS One **4:**e5466. http://dx.doi.org/10.1371/journal.pone.0005466.
33. **Huang Y, Liu H, Li S, Tang Y, Wei B, Yu H, Wang C.** 2014. MAVS-MKK7-JNK2 defines a novel apoptotic signaling pathway during viral infection. PLoS Pathog **10:**e1004020. http://dx.doi.org/10.1371/journal.ppat.1004020.
34. **Li XD, Sun L, Seth RB, Pineda G, Chen ZJ.** 2005. Hepatitis C virus protease NS3/4A cleaves mitochondrial antiviral signaling protein off the mitochondria to evade innate immunity. Proc Natl Acad Sci U S A **102:**17717–17722. http://dx.doi.org/10.1073/pnas.0508531102.
35. **Peters K, Chattopadhyay S, Sen GC.** 2008. IRF-3 activation by Sendai

virus infection is required for cellular apoptosis and avoidance of persistence. J Virol **82:**3500–3508. http://dx.doi.org/10.1128/JVI.02536-07.

36. **Yang K, Shi H, Qi R, Sun S, Tang Y, Zhang B, Wang C.** 2006. Hsp90 regulates activation of interferon regulatory factor 3 and TBK-1 stabilization in Sendai virus-infected cells. Mol Biol Cell **17:**1461–1471. http://dx.doi.org/10.1091/mbc.E05-09-0853.
37. **Schulte TW, Akinaga S, Soga S, Sullivan W, Stensgard B, Toft D, Neckers LM.** 1998. Antibiotic radicicol binds to the N-terminal domain of Hsp90 and shares important biologic activities with geldanamycin. Cell Stress Chaperones **3:**100–108. http://dx.doi.org/10.1379/1466-1268(1998)003<0100:ARBTTN>2.3.CO;2.
38. **Stebbins CE, Russo AA, Schneider C, Rosen N, Hartl FU, Pavletich NP.** 1997. Crystal structure of an Hsp90-geldanamycin complex: targeting of a protein chaperone by an antitumor agent. Cell **89:**239–250. http://dx.doi.org/10.1016/S0092-8674(00)80203-2.
39. **Clark K, Plater L, Peggie M, Cohen P.** 2009. Use of the pharmacological inhibitor BX795 to study the regulation and physiological roles of TBK1 and IkappaB kinase epsilon: a distinct upstream kinase mediates Ser-172 phosphorylation and activation. J Biol Chem **284:**14136–14146. http://dx.doi.org/10.1074/jbc.M109.000414.
40. **Lin RT, Heylbroeck C, Pitha PM, Hiscott J.** 1998. Virus-dependent phosphorylation of the IRF-3 transcription factor regulates nuclear translocation, transactivation potential, and proteasome-mediated degradation. Mol Cell Biol **18:**2986–2996.
41. **Chattopadhyay S, Marques JT, Yamashita M, Peters KL, Smith K, Desai A, Williams BRG, Sen GC.** 2010. Viral apoptosis is induced by IRF-3-mediated activation of Bax. EMBO J **29:**1762–1773. http://dx.doi.org/10.1038/emboj.2010.50.
42. **Fan AC, Kozlov G, Hoegl A, Marcellus RC, Wong MJ, Gehring K, Young JC.** 2011. Interaction between the human mitochondrial import receptors Tom20 and Tom70 in vitro suggests a chaperone displacement mechanism. J Biol Chem **286:**32208–32219. http://dx.doi.org/10.1074/jbc.M111.280446.
43. **Hemmi H, Takeuchi O, Sato S, Yamamoto M, Kaisho T, Sanjo H, Kawai T, Hoshino K, Takeda K, Akira S.** 2004. The roles of two I kappa B kinase-related kinases in lipopolysaccharide and double stranded RNA signaling and viral infection. J Exp Med **199:**1641–1650. http://dx.doi.org/10.1084/jem.20040520.
44. **Petrasek J, Iracheta-Vellve A, Csak T, Satishchandran A, Kodys K, Kurt-Jones EA, Fitzgerald KA, Szabo G.** 2013. STING-IRF3 pathway links endoplasmic reticulum stress with hepatocyte apoptosis in early alcoholic liver disease. Proc Natl Acad Sci U S A **110:**16544–16549. http://dx.doi.org/10.1073/pnas.1308331110.
45. **Brubaker SW, Gauthier AE, Mills EW, Ingolia NT, Kagan JC.** 2014. A bicistronic MAVS transcript highlights a class of truncated variants in antiviral immunity. Cell **156:**800–811. http://dx.doi.org/10.1016/j.cell.2014.01.021.